Supplementary materials of: Formation of glacier tables caused by differential ice melting

Marceau Hénot,[1] Vincent Langlois,[2] Nicolas Plihon,[1] and Nicolas Taberlet[1,*]

[1] *Univ Lyon, ENS de Lyon, Univ Claude Bernard, CNRS, Laboratoire de Physique, F-69342 Lyon, France*

[2] *Laboratoire de Géologie de Lyon, Terre, Planètes, Environnement, Department of Earth Science, Université Claude Bernard Lyon 1, France*

FIG. S1. Pictures of rocks 1 to 4 (see table 1 of the main text) at the begining and at the end of the observation.

Air temperature measurement on site and at the automated Requin weather station. The model used in the article relies on meteorological data measured at the Requin automatic weather station (AWS) located on the edge of the glacier approximately 3 km away from the table measurement site (see fig. 2a of the main text) and 800 m higher in altitude. While we do not expect the solar irradiation or the wind velocity to change much between these two locations, the air temperature is likely to be affected by the altitude difference as well as the proximity of the glacier. Between 18/06/2021 and 06/07/2021 we measured the air temperature 3 m above the glacier surface at the table measurement site using a thermocouple and a home-made autonomous recording device. These data are plotted in fig. S2a alongside with the data from the Requin AWS. This shows that the air temperature onsite can be deduced from the Requin AWS data by adding a 2.5°C offset (see fig. S2b and c).

Adjustement of ice albedo and turbulent heat exchange coefficient. The ablation rate $\Delta\dot{z}$ of the ice surface on location 3 during period A was computed from the data of fig. 4a of the main text and is shown in fig. S3a. The parameters of the model α_{ice} and $\mathcal{C}$ were adjusted by minimising the mean squared deviation from the model (MSD) as shown in fig. S3c. The modeled ablation rate obtained with the best parameter values ($\alpha_{\text{ice}} = 0.33$ and $\mathcal{C} = 2.3$ W$\cdot$K$^{-1}\cdot$m^{-1}) is shown in fig. S3a and b as a function of the measured ablation rate.

Assumption on area of contact between the rock and the ice. In our model, the contact area A_{base} between the rock and the ice is assumed to stay constant equal to its initial value $A^0_{\text{base}} = d_1 d_2$. This simple hypothesis needs to be discussed as that this area clearly diminishes as the ice foot grows (see for instance fig. 1c of the main text). For rock 1, the area is almost divided by two after 200 h. By letting the contact area be diminished by a factor f ($A_{\text{base}} = f A^0_{\text{base}}$) the model developed in the article yields the same results as long as the aspect ratio of the rock is replaced by an effective aspect ratio $\beta_{\text{eff}} = \beta + f/4$. For rock 1 ($\beta = 0.23$), with $f = 0.5$, this leads to $\beta_{\text{eff}} = 0.36$. Yet, as visible in fig. 6 of the main article, in the table formation regime, the ratio $\langle H/H_{\text{ice}}\rangle$ and thus the ice foot

* Corresponding author: nicolas.taberlet@ens-lyon.fr

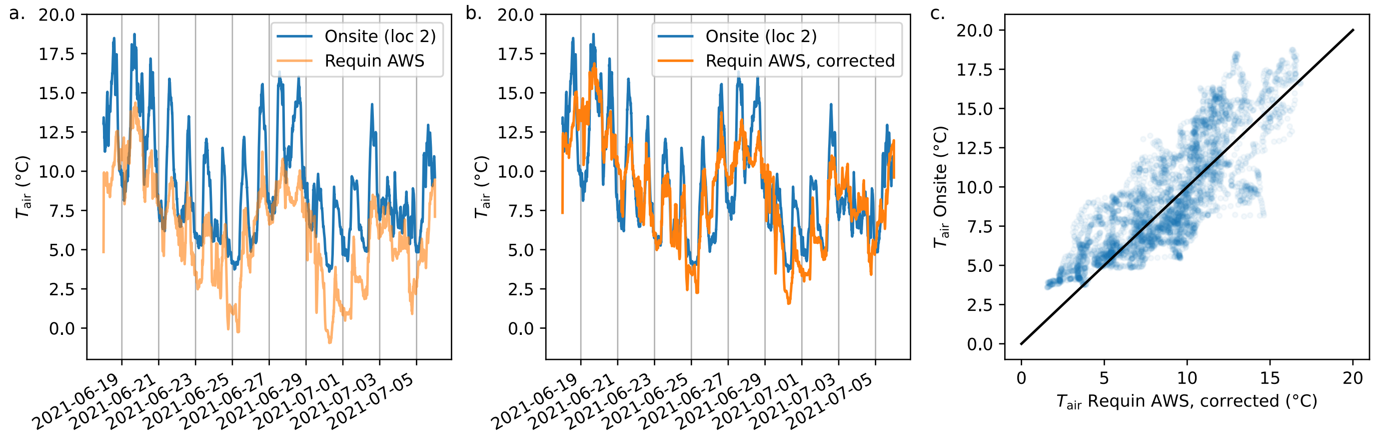

FIG. S2. (a, b) Air temperature T_{air}, 3 m above the ground surface, measured at the Requin AWS (light orange on a) and on the table measurement site (blue) (see location 2 in fig. 2 of the main text). The difference in location and altitude can be taken into account by correcting the AWS data by adding an 3°C offset (orange on b). (c) T_{air} measured on site versus corrected from the AWS data.

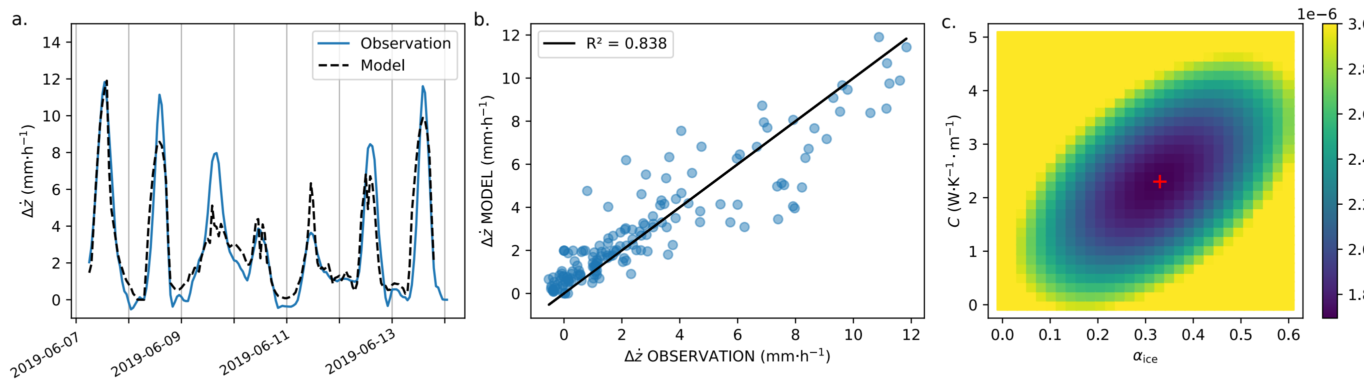

FIG. S3. (a) Ablation rate of the glacier surface on location 3 during period A. (b) Modeled versus measured ablation rate for the adjusted parameters $\alpha_{\mathrm{ice}} = 0.33$ and $\mathcal{C} = 2.3$ W·K^{-1}·m^{-1}. (c) Sensibility on the MSD of the adjustable parameters $\mathcal{C}$ and α_{ice}. The red cross corresponds to the best parameters.

growth dynamics, only show a weak dependence with the aspect ratio (of the order of the error bar) which justify the simple assumption.

Assumption on the rock area illuminated by the sun. In our model, we assume that, on average, the solar irradiation Φ is received by a rock on an area $\langle A_{\mathrm{sun}}\rangle = d_1 d_2$ corresponding to the surface area of the top of the rock. In the following we discuss this assumption. Let us consider a 2D rock (see fig. S4a) of height e and width d illuminated by a solar irradiation Φ and let θ be the angle between the sun direction and the vertical direction. The heat flux (per unit of depth) received by the rock from the sun is:

$$q_{\mathrm{sun}\to\mathrm{rock}}(\theta) = \Phi d\left[\cos\theta + \beta\sin\theta\right] \tag{1}$$

where $\beta = e/d$ is the aspect ratio of the rock. During a day, the angle θ goes to $-\theta_0$ to θ_0. The mean heat flux is:

$$\langle q_{\mathrm{sun}\to\mathrm{rock}}\rangle = \frac{1}{\theta_0}\int_0^{\theta_0} q_{\mathrm{sun}\to\mathrm{rock}}(\theta)\mathrm{d}\theta = \Phi d\left[\sin\theta_0 + \beta(1-\cos\theta_0)\right] \tag{2}$$

As shown in fig S4b, for $\theta_0 = 75°$ and a rock aspect ratio β lying between 0.1 and 0.8, the result of eq 2 differs from Φd by less than 20 %, which justifies the assumption made in the model.

Granite albedo. The spectral reflectivity $R(\lambda)$ of weathered granite was measured by [1] between $\lambda_1 = 400$ nm and $\lambda_2 = 750$ nm. We used this data to compute the granite albedo:

$$\alpha_{\mathrm{granite}} = \frac{\int_{\lambda_1}^{\lambda_2} R(\lambda)\Phi(\lambda)\mathrm{d}\lambda}{\int_{\lambda_1}^{\lambda_2}\Phi(\lambda)\mathrm{d}\lambda} \quad , \quad \Phi(\lambda) \propto \frac{1}{\lambda^5}\frac{1}{e^{hc/(\lambda kT)}-1} \tag{3}$$

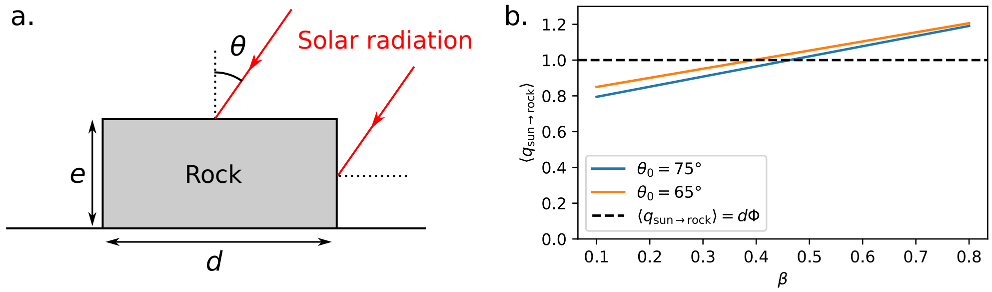

FIG. S4. (a) Schematics of a rock receiving solar irradiation. (b) Mean heat flux received by the rock from the sun given by eq. 2 (solid lines). The dashed line corresponds to the assumption made in the model.

where $\Phi(\lambda)$ is the spectral distribution of the solar radiation, estimated from Planck's law. h is the Planck constant, c the speed of light, k the Boltzmann constant and $T = 5780$ K the sun surface temperature. This leads to $\alpha_{\mathrm{granite}} = 0.18$.

Ice ablation during period C: from 27/05 to 03/06/2021.

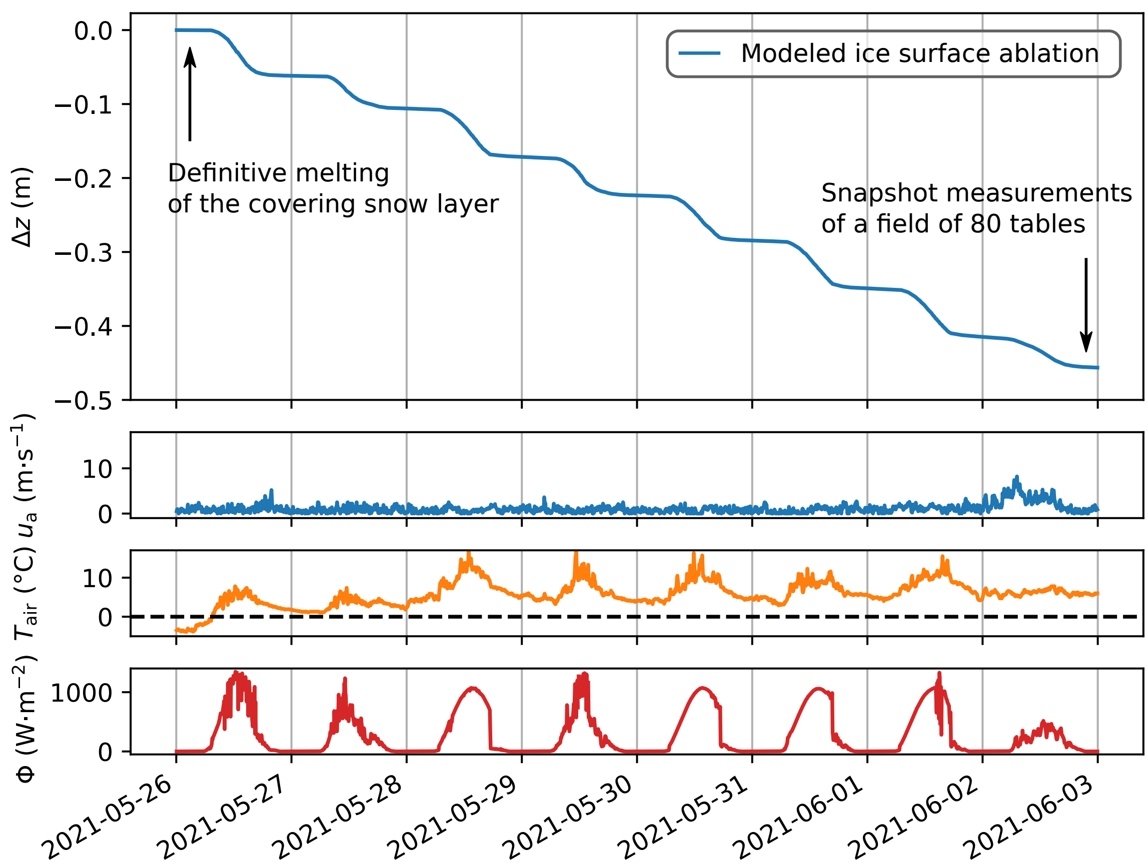

FIG. S5. Model for ice ablation Δz during period C given by eq. 2 of the main text with parameters specified in the caption of fig. S3 and using the meteorological data shown (wind speed u_{a}, air temperature T_{air} and solar radiation Φ). The beginning of period C was determined from the observation made using the Montenvers webcam [2] that the covering snow layer (on location 1 in fig. 2a of the main text) definitively melted on 27 May 2021. The meteorological data used as input of the model are shown (wind speed u_{a}, air temperature T_{air} and solar radiation Φ).

[1] R. D. Watson, Spectral reflectance and photometric properties of selected rocks, Remote Sensing of Environment **2**, 95 (1971).
[2] Montenvers webcam, https://www.bergfex.fr/chamonix-mont-blanc/webcams/c3944/ (2021).